Pages: 34-46 / Vol. 17- No. 1/Winter- Spring 2024

Journal of Aerospace Science and Technology

Journal Homepage: www:jast.ias.ir

Original Research Article

Optimal Strategy for Multi-agent Mission Segregation: Search and Coverage Application

Benyamin Ebrahimi [1] *, Jafar Roshanian, Ali Asghar Bataleblu

1-2-Intelligent Control Systems Institute, K.N. Toosi University of Technology, Tehran, Iran
3- Faculty of Engineering, Free University of Bolzano Bozen, Bolzano, Italy

Article History:
Received: 25. June. 2023
Revised: 01.December.2023
Accepted: 11. September.2023

Keywords: *Optimization, Multi-agent system, Environment division, Cooperative search and coverage*

DOI : doi.org/10.22034/jast.2023.403842.1156

ABSTRACT

Significant attention has been given to the field of multi-agent systems in recent years due to its potential to solve complex problems that cannot be addressed by a single agent. One such problem is the cooperative search and coverage application, which requires multiple agents to efficiently search and cover a given area. However, the effectiveness of such systems is dependent on various factors, including mission definition parameters and the approach used to achieve mission performance optimality. In this paper, an optimal strategy for segregating multi-agent missions for search and coverage applications is proposed. The proposed strategy involves dividing a single mission into several simultaneous missions based on the optimal division of the environment that ensures system performance optimality while achieving a common goal. The mission area is divided into sub-areas, and each sub-area is assigned to specific agents to improve overall system performance. The effectiveness of the proposed strategy is demonstrated through simulations and relevant comparisons.

Introduction

The use of multi-agent systems has gained significant attention due to their capabilities in various applications. In particular, employing multiple robots equipped with advanced sensors and communication equipment for cooperative search and coverage in a given region can significantly increase the likelihood of mission success. This paper focuses on the multi-agent cooperative search and coverage (MACSC) application where a team of robots aims to find several unknown targets scattered in a given surveillance region while minimizing uncertainty [1- 3]. In this mission, each robot maintains an individual probability map that is updated based on information gathered from its sensors. The probability maps are then shared and fused with neighboring robots to update each other's maps. By integrating the fused information into the cooperative path-planning strategy, robots converge to regions with a high probability of target existence to find targets and reduce uncertainty. Therefore, addressing issues related to the environment, information fusion, and path planning are crucial in solving cooperative search and coverage problems. The environment in which agents operate can be represented by a map that serves as their knowledge base. To create this map, the search area is divided into smaller cells, each associated with probability or uncertainty values. While most research assumes a convex polygon environment, some studies consider more complex and realistic environments with obstacles. Each robot updates its search map based on its sensory information, but the best overall knowledge of the search region can only be obtained through the fusion of exchanged sensory information with other robots. Bayesian theory [4] and Dempster-Shafer theory [5, 6] are commonly used fusion

1 (Corresponding Author), Benyamin Ebrahimi, Assistan Professor , Email: mr.ghafari@arakut.ac.ir

Print ISSN:1735-2134 Online ISSN: 2345-3648

strategies. Two evidential map-building approaches based on these theories were proposed in [7] for multi-robot cooperative search and coverage in an uncertain environment. In another study [8], a consensus-like distributed fusion scheme was proposed to fuse the probability maps of robots after linearizing the Bayesian update and introducing a nonlinear transformation of the probability map to simplify computation.

The efficiency of the Cooperative Search and Coverage (CSC) problem heavily relies on the path planning for multi-agents [9]. This can be formulated as an optimization problem that aims to minimize or maximize the team objective function while taking into account a set of equality and/or inequality constraints. To date, various methods have been explored to improve agent path planning, including Dynamic Programming (DP) [2, 10], Neural Networks (NNs) [11], and Reinforcement Learning (RL) [12-14], gradient-based optimization [15, 16], Artificial Potential Field (APF) [17, 18], Meta-heuristic optimization algorithms [19-21], and Model Predictive Control (MPC) [22, 23] which is also known as Receding Horizon Control (RHC). For instance, a distributed gradient-based optimization approach that considers overloading constraints and collision avoidance has been proposed for path planning in multi-agent cooperative search scenarios [24]. In [22], a three-layer mission planning system has been designed for distributed cooperative search and coverage. This system uses a Receding Horizon Predictive Control algorithm to ensure optimal path planning while considering collision avoidance and flying robots' communications. During CSC missions, each agent utilizes a probability map that is continuously updated through information gathered from the agent's sensors and shared with neighboring agents. The objective is to converge on regions with high probabilities of target existence to effectively reduce uncertainty in the search area. While these methods may enhance system performance, they do not guarantee optimality.

To address this issue, this paper proposes an optimal strategy for multi-agent systems in cooperative CSC by dividing the mission into four sub-missions based on the environment. The proposed approach aims to leverage the high capability of multi-agent systems in cooperative tasks. It should be noted that although the presented methods and strategies for multi-agent missions such as search and coverage may improve system performance, they do not necessarily ensure performance optimality.

The rest of this paper is organized as follows. In the next section, the definition of multi-agent CSC is provided. The proposed strategy is discussed in section 3. The numerical simulations and comparisons that verify the proposed approach are provided in section 4. To sum up, the conclusions are drawn in section 5.

Multi-agent CSC

The search region $\mathcal{O} \in \mathbb{R}^2$ is assumed to be a continuous convex polygon with the area of $L \times W$ in 2D Euclidean space. In this study, it is presumed that the search area can be partitioned into 4 sub-area $\mathcal{O}_s \in \mathcal{O} \in \mathbb{R}^2$ with the area of $l_s \times w_s$ determined through an optimization process. As shown in Figure 1, the search area is uniformly divided into m cells with the size of $\delta = \Delta x \times \Delta_y$ and with this cell size, the sub-regions would be divided into m_s cells. Δx and Δ_y denote the length and width of the cell, respectively. Each cell c is identified with its center $\mu_c = [x_c, y_c]^T$, where x_c and y_c are the coordinates of its center. In the search region, each cell is associated with a probability of target existence $P_{i,k}(\theta_c)$ within the cell at moment k, modeled as a Bernoulli distribution. In which $\theta_c \in \{0,1\}$ is the target existence in cell c, i.e, $\theta_c = 1$ and $\theta_c = 0$ reveal the target and no target presence in cell c, respectively. In this work, no threats and obstacles are considered in the search region, and at most, just one target could be located in each cell.

The kinematics model [24] for the flying robots is defined as $\dot{\mathbf{s}}_i = [\dot{x}_i, \dot{y}_i, \dot{\psi}_i, \dot{v}_i]^T = [v_i \cos\psi_i, v_i \sin\psi_i, u_i, 0]^T$, with $[x_i, y_i]^T$ representing the planar position of the ith robot, ψ as the heading angle, and v as the flight velocity. The action variable u corresponds to the flying robot turn rate command,$\dot{\psi}$.

It is assumed that the agents are equipped with airborne image sensors that have the same sensing radius $R_s = h \tan\varphi$, forming a circular field of view (FOV). Here, h and φ indicate the flight altitude and half-angle of the sensor's field of view, respectively [24].

$$\mathbb{C}_{i,k} = \{\boldsymbol{\xi} \in \mathcal{O} | \, \|\boldsymbol{\xi} - \boldsymbol{\mu}_{i,k}\| \leq \boldsymbol{R_s}\} \quad (1)$$

The position of the ith agent at time k is denoted by $\mu_{i,k}$, and ξ indicates an arbitrary point within the search region. At time k, the network topology is modeled as an undirected graph $\boldsymbol{\mathcal{G}_k} = (\boldsymbol{\mathcal{E}_k}, \boldsymbol{\mathcal{V}})$,

where the vertices set $\boldsymbol{\mathcal{V}}$ includes $\{1,2,\dots,N\}$, and the edge set $\boldsymbol{\mathcal{E}}_k$ includes $\{\{i,j\}: i,j \in \mathcal{V}; \|\boldsymbol{\mu}_{i,k} - \boldsymbol{\mu}_{j,k}\| \leq R_c\}$, with R_c denoting the communication range assumed to be large enough for all UAVs to maintain communication throughout the environment in this paper.

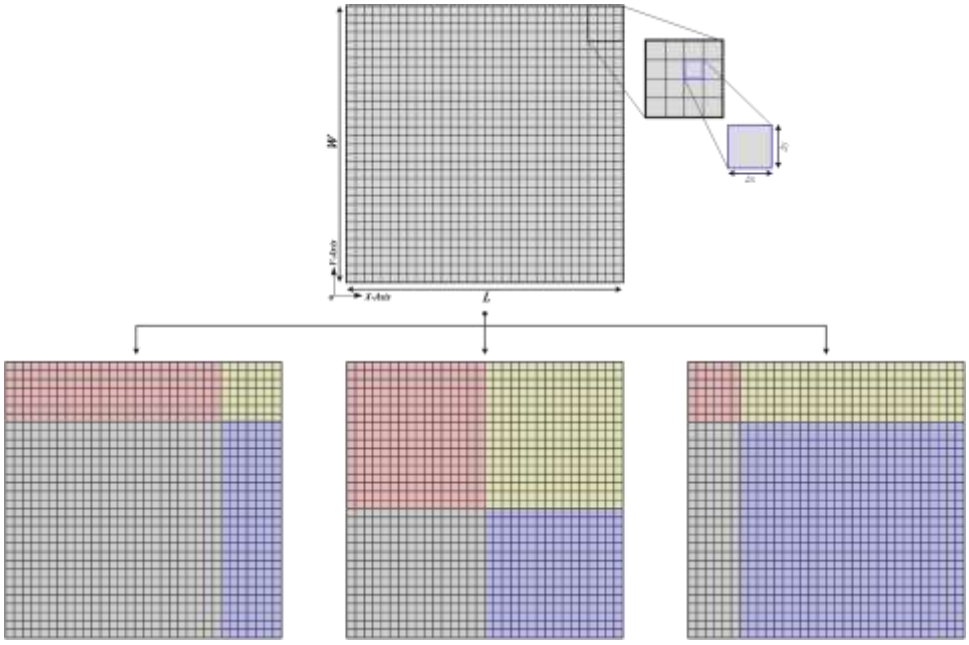

Figure 1. Environment

During the mission, each agent updates its probability map ($\mathcal{P}_{i,c,k} \triangleq \mathcal{P}_{i,k}(\theta_c)$) using the Bayesian rule [8, 23]. This process incorporates sensor characteristics $P(Z_{i,c,k}|\theta_c)$, sensor observations $Z_{i,c,k}$, and prior probability maps.

$$\mathcal{P}_{i,c,k} = \begin{cases} \dfrac{p\mathcal{P}_{i,c,k-1}}{p\mathcal{P}_{i,c,k-1} + q(1-\mathcal{P}_{i,c,k-1})} & ,Z_{i,c,k}=1 \\ \dfrac{(1-p)\mathcal{P}_{i,c,k-1}}{(1-p)\mathcal{P}_{i,c,k-1} + (1-q)(1-\mathcal{P}_{i,c,k-1})} & ,Z_{i,c,k}=0 \\ \mathcal{P}_{i,c,k-1} & otherwise \end{cases} \quad (2)$$

Sensor observations can indicate target or non-target detection, with $Z_{i,c,k} \in \{0,1\}$, representing $Z_{i,c,k}=1$ for target detection and $Z_{i,c,k}=0$ for non-target detection. The probability of target existence within cell c at moment k is denoted as $P_{i,c,k}$. Additionally, $P(Z_{i,c,k}=1|\theta_c=1)=p$ represents detection probability, and $P(Z_{i,c,k}=1|\theta_c=0)=q$ represents false alarm probability, both of which are constant and known for all cells and agents.

$$\begin{aligned} \mathcal{Q}_{i,c,k} &\triangleq \ln\left(\frac{1}{\mathcal{P}_{i,c,k}} - 1\right) \\ \mathcal{Q}_{i,c,k} &= \mathcal{Q}_{i,c,k-1} + v_{i,c,k} \end{aligned} \quad (3)$$

where

$$v_{i,c,k} = \begin{cases} \ln\dfrac{q}{p} & ,Z_{i,c,k}=1 \\ \ln\dfrac{1-q}{1-p} & ,Z_{i,c,k}=0 \\ 0 & otherwise \end{cases} \quad (4)$$

The probability map is updated using a nonlinear transformation and shared among agents through map fusion, following a consensus protocol where each vehicle exchanges its updated probability map with nearby agents $H_{i,c,k}$.

$$\begin{aligned} H_{i,c,k} &= \mathcal{Q}_{i,c,k-1} + v_{i,c,k} \\ \mathcal{Q}_{i,c,k} &= \sum_{j=1}^{N} \omega_{i,j,k} H_{j,c,k} \end{aligned} \quad (5)$$

where $\omega_{i,j,k} = 1 - ((n_{i,k}-1)/N)$, $\omega_{i,j,k} = (1/N)$ for $j \in \mathcal{N}_{i,k}$, $\omega_{i,j,k} = 0$ for $j \notin \mathcal{N}_{i,k}$, see [8, 25].

To find targets in a given area and decrease the uncertainty of the area, a path-planning approach is employed to control agents. The distributed gradient optimization technique introduced in [24] is utilized for this purpose. The method defines an equation to quantify uncertainty by using a probability map. A cell is deemed to have a target presence if $P_{i,c,k}$ gets close to 1, while a probability of 0 indicates no target's presence. When uncertainty prevails with a probability of 0.5, it is considered the highest. The uncertainty map of the ith agent at k instant is denoted by $\phi_{i,k}$, where k_ϕ is a gain parameter. The objective function of the problem, which is the coverage performance, is defined in terms of Voronoi regions denoted by V_i.

$$\phi_{i,k}(c) = e^{-k_\phi \left|\ln\left(\frac{P_{i,c,k}}{1-P_{i,c,k}}\right)\right|} \triangleq e^{-k_\phi |Q_{i,c,k}|} \quad (6)$$

$$J(\boldsymbol{\mu}_k, \boldsymbol{u}_k, \boldsymbol{\phi}_k) = \sum_{i=1}^{N} \int_{V_i} \left\| \boldsymbol{\mu}_{i,k+1} - \boldsymbol{\xi} \right\|^2 \phi_{i,k}(\boldsymbol{\xi}) d\boldsymbol{\xi} \quad (7)$$

The position and control input of the ith agent at k time are represented by $\boldsymbol{\mu}_k$ and $\boldsymbol{u}_k$, respectively. The Mass A_i, and centroid C_{v_i} of each Voronoi region can be computed through the equations presented in [24] and [26]. The following equation approximates the Voronoi areas using a discrete method, where δ represents each cell's area.

$$A_i \triangleq \int_{V_i} \phi_{i,k}(\boldsymbol{\xi})\, d\boldsymbol{\xi},\ C_{V_i} \triangleq \frac{\int_{V_i} \xi . \phi_{i,k}(\xi) d\xi}{A_i} \quad (8)$$

$$A_i \triangleq \int_{V_i} \phi_{i,k}(\boldsymbol{\xi})\, d\boldsymbol{\xi} = \sum_{V_i} \phi_{i,k}(c)\delta\,,$$
$$C_{V_i} \triangleq \frac{\int_{V_i} \xi . \phi_{i,k}(\xi) d\xi}{A_i} = (1/A_i) \sum_{V_i} \boldsymbol{\mu}_c \phi_{i,k}(c)\delta \quad (9)$$

The optimal control input vector ($\boldsymbol{u}_k^*$) can be obtained by solving the optimal control problem of minimizing $J(\boldsymbol{\mu}_k, \boldsymbol{u}_k, \boldsymbol{\phi}_k)$. The first-order gradient optimization algorithm is used to minimize the objective function $\boldsymbol{u}_k^* = \arg\min J(\boldsymbol{\mu}_k, \boldsymbol{u}_k, \boldsymbol{\phi}_k)$, as described in [16, 24 and 27].

The optimal solutions updated by the equation $u_{i,k+1} = u_{i,k} - \gamma_i(\partial J/\partial u_i)(\boldsymbol{u}_k)$ are obtained by applying the first-order gradient optimization algorithm to minimize the objective function J (for more details, see ref [16, 24 and 27]. One way to apply the control input, which is subject to the maneuverability constraint of $-\dot{\psi}_{max} \le u_i \le \dot{\psi}_{max}$, is by incorporating the constrained factor C_u for the control variable $\hat{u}_i \in \mathbb{R}$.

$$u_i = C_u \hat{u}_i = \begin{cases} -\dot{\psi}_{max} & \hat{u}_i \le -\dot{\psi}_{max} \\ \hat{u}_i & -\dot{\psi}_{max} \le \hat{u}_i \le \dot{\psi}_{max} \\ \dot{\psi}_{max} & \hat{u}_i \ge \dot{\psi}_{max} \end{cases} \quad (10)$$

Optimal Strategy (Segregation)

The optimization of mission segregation would be a practical step toward achieving successful multi-agent system performance. To accomplish this, an optimal strategy based on dividing the area according to the overall performance of the multi-agents must be adopted. This section proposes a strategy for segregating the mission into four submissions.

In defining the sub-areas, the approach adopted is based on the segregation provided in Figure 2. The entire mission is split into four sub-missions, each assigned a specific area. The agents assigned to each sub-mission will start their operation from different sides of the environment.

This strategy ensures that the agents will cover the entire assigned area more efficiently, reducing redundancy and avoiding the need for a crossover in the scale of the original area (not sub-area). Each set of agents within their assigned sub-area will autonomously complete their specific task and return to their original position while developing the performance of the common mission. Through this strategy, there is the chance of increasing the efficiency and effectiveness of the multi-agent system.

In this study, we will discuss an optimization problem that aims to minimize the number of agents while maximizing the uncertainty ratio.

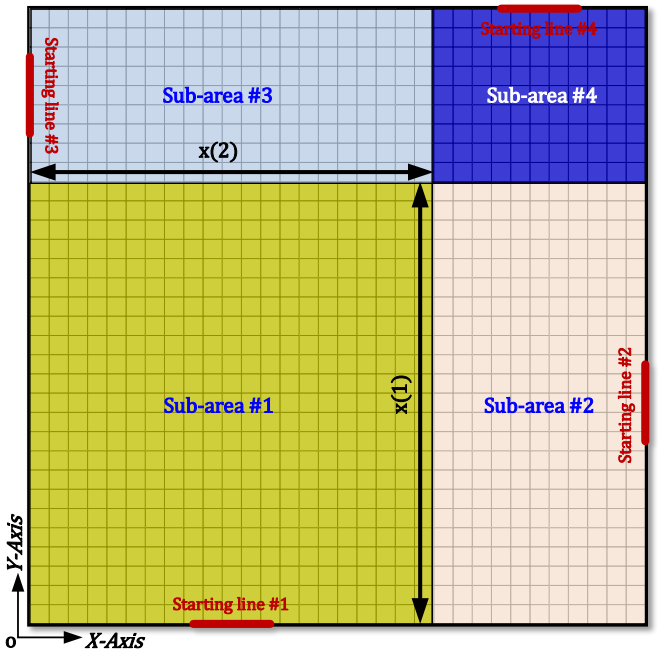

Figure 2. Region Segregation.

The objective of this optimization problem is twofold (Table 1): first, to minimize the overall number of agents required to complete a mission; and second, to maximize the uncertainty ratio. The uncertainty ratio is defined as the ratio between the region covered by the agents in each sub-region and the total region of interest.

Table 1. Objective Functions.

Objective Function	
functions	**formula**
min . Number of Agents	$f_1(\mathbf{x}): \sum_{i=1}^{4} N_{S_i}$
max . Uncertainty Ratio	$f_2(\mathbf{x}): \sum_{i=1}^{2} \varrho_{S_i}$

Let $\varrho_{S_i} = \left(\left(1 - \bar{\phi}_{S_i,k=t_f}\right) * \bar{\phi}_{S_i,k=0}\right) / \bar{\phi}_{k=0}$ denote the uncertainty ratio of ith sub-region ($\bar{\phi}_{S_i,k}$) to whole search region $\bar{\phi}_k$. To achieve these objectives, several design variables (**Error! Not a valid bookmark self-reference.**) need to be considered. These include parameters for defining sub-areas, such as their size and shape; operational parameters for each agent, such as velocity and initial head angle; and finally, the number of agents required for each set.

Table 2. Design Variables.

Design Variables						
type	Parameters		Sym.	X	LB	UB
discrete	Sub-area size parameter: number of cells in X-Axis		n_{CX}	$x(1)$	40	160
discrete	Sub-area size parameter: number of cells in Y-Axis		n_{CY}	$x(2)$	40	160
discrete	Number of Agents Sub-area #1		N_{S_1}	$x(3)$	3	20
discrete	Number of Agents Sub-area #2		N_{S_2}	$x(4)$	3	20
discrete	Number of Agents Sub-area #3		N_{S_3}	$x(5)$	3	20
discrete	Number of Agents Sub-area #4		N_{S_4}	$x(6)$	3	20
continuous	Agents initial head angle (deg)	*on side* #1: [45,135]	ψ_0	$x(7)$	0	90
		on side #2: [135,225]				
		on side #3: [225,315]				
		on side #4: [−45,45]				
continuous	Agents velocity (m/s)		v	$x(8)$	40	75

However, these design variables must satisfy certain constraints (Table 3) to ensure that they meet performance criteria while executing their mission. These constraints are assumed as follows:

Table 3. Constraints.

Constraints	
functions	formula
$g_1(x)$	$\sum_{i=1}^{4} \frac{\bar{\varphi}_{S_i,k=t_f}}{\bar{\varphi}_{S_i,k=0}} \leq 0.5$
$g_2(x)$	$\frac{\sum_{i=1}^{4} N_{DT_{S_i}}}{\lfloor .N_T \rfloor} \geq 0.6$

in which N_{DT_S} indicates the number of the detected targets by each set of agents in their sub-regions, and the number of all targets in the whole area is denoted by N_{T}.

Simulations, Results, and Comparison

The proposed scenario aims to evaluate the effectiveness of optimal solutions in carrying out cooperative search and coverage missions within a designated time limit. To showcase the proposed method for distributed cooperative search and coverage application, MATLAB® software was utilized to run simulations. The goal is to determine the efficiency of the optimal solutions and their potential to accomplish the task.

As shown in Figure 3, the surveillance area is defined to have a size of $10 \times 10\ km^2$, and it has been divided into uniform cells of $50 \times 50\ m^2$. Within this vast area, there are a total of 80 targets (green circle) that have been randomly scattered throughout the surveillance area and the locations of these targets are unknown. To generate the probability map, the Gaussian distribution function $Q(\xi) = (1/\sigma\sqrt{2\pi})e^{-(\xi-\mu)^2/2\sigma^2}$ with a mean value μ indicating the expected location and a standard deviation σ has been applied. In this case, the Gaussian distribution function is being used to determine the probability of the targets being present within the surveillance area.

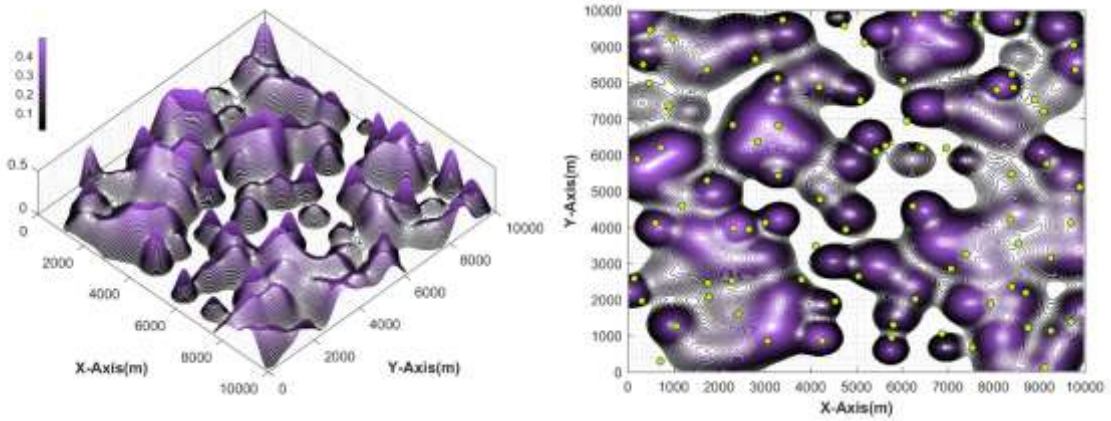

Figure 3. left) probability distribution, right) location of targets.

In this simulation, the probability of detection is set at 0.9, which means that the targets have a high chance of getting detected when they are present in the field of view. The false alarm probability is considered to be 0.1, which means that there is a relatively low possibility of getting false alarms from the environment.

Furthermore, the simulation has been run for a specific amount of time, with the given period being 120 seconds. This means that any targets that are present in the monitored area during this time frame will be detected with a high degree of accuracy, provided that they are within the field of view of the sensors. The maximum turning angle has been set at 0.3 radians and the half-angle of FOV has been set at 0.4 radians, which means that the sensors have a relatively narrow field of view.

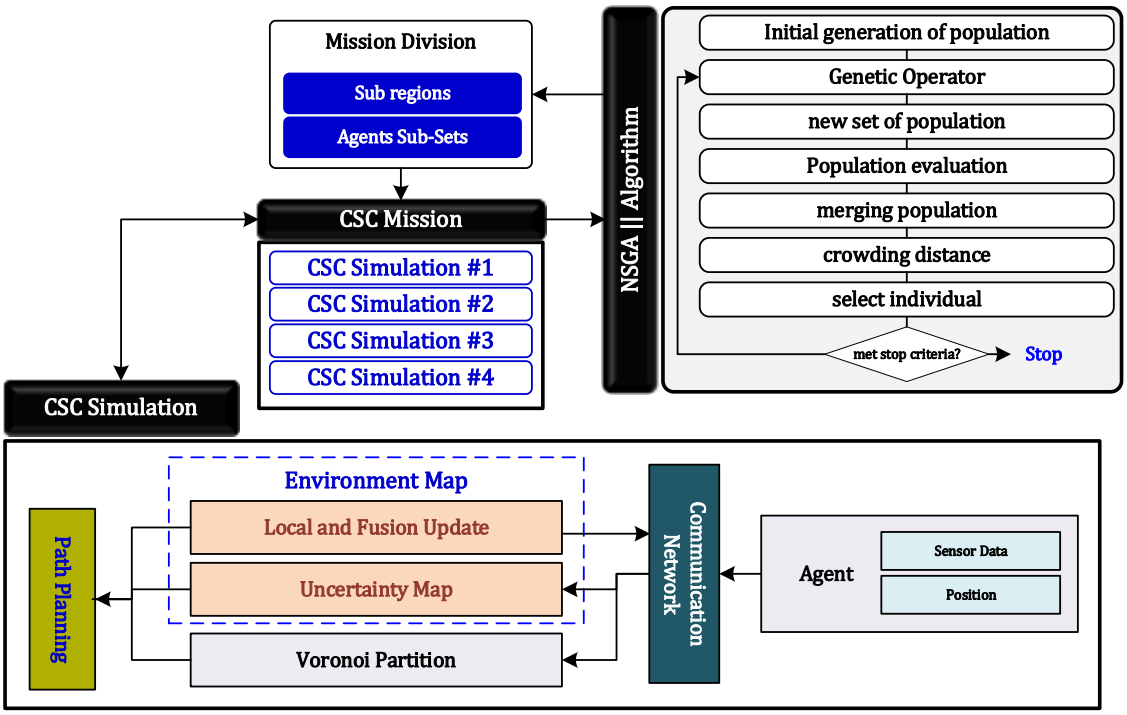

Figure 4. Proposed Strategy.

To find multi-objective trade-off optimal solutions (Pareto frontier), the non-dominated sorting genetic algorithm (NSGA II) [28] was applied in the simulation. As shown in Figure 4, in each iteration of the optimization process, the optimizer returns values of the new set of design variables (DVs) to define the mission parameters and mission division. During each sub-mission, the agents' sensor measurements will update the local probability map. The probability map for each sub-region can be updated by fusing shared information through the communication network between the sets of agents assigned to that region. This process allows for an uncertainty map to be obtained. Additionally, by utilizing shared information between agents in each sub-region, the Voronoi partition of the environment can be updated. As a result, each agent in every sub-mission is directed to cover their designated sub-region and locate targets using a path planning policy.

The parameters used for NSGA II were a crossover fraction of 0.8 and a mutation fraction of 0.2. The simulation was run for 30 generations with a population size of 50. The optimal solutions obtained from the simulation include feasible solutions and the Pareto frontier, which are depicted in Figure 5.

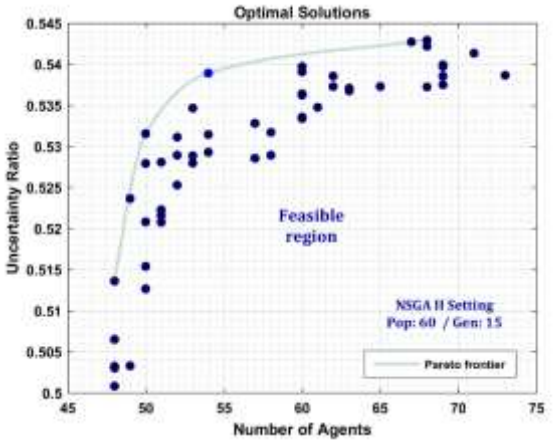

Figure 5. Optimal Solution.

To evaluate the effectiveness of the optimal strategy, the performance of the CSC mission associated with one
the selected point from the Pareto frontier is analyzed. The optimal design variables and objective functions associated with this point are presented in
Table 4 and **Error! Reference source not found.**, respectively.

Table 4. Optimal Solution: Objective Functions.

Objective Function	
functions	formula
min . Number of Agents	$f_1(\mathbf{x}): 54$
max . Uncertainty Ratio	$f_2(\mathbf{x}): 53.89$

Design Variables					
type	Parameters		Sym.	X	value
discrete	Sub-area size parameter: number of cells in X-Axis		n_{CX}	$x(1)$	160
discrete	Sub-area size parameter: number of cells in Y-Axis		n_{CY}	$x(2)$	112
discrete	Number of Agents Sub-area #1		N_{S_1}	$x(3)$	16
discrete	Number of Agents Sub-area #2		N_{S_2}	$x(4)$	14
discrete	Number of Agents Sub-area #3		N_{S_3}	$x(5)$	15
discrete	Number of Agents Sub-area #4		N_{S_4}	$x(6)$	9
continuous	Agents initial head angle (deg)	$on\ side$ #1: $[45,135]$	ψ_0	$x(7)$	60.2014
		$on\ side$ #2: $[135,225]$			
		$on\ side$ #3: $[225,315]$			
		$on\ side$ #4: $[-45,45]$			
continuous	Agents velocity (m/s)		v	$x(8)$	72.6563

The study presented in this article focuses on the performance of a system during a mission. The simulation results provide valuable insights into the effectiveness of the system in reducing uncertainty and finding targets. The paths of the agents and mean uncertainty reduction in each sub-region are depicted in Figure 6, which clearly shows the success of the system. One interesting observation from Figure 6 is that the sub-regions 1 to 4, corresponding to the selected optimal point, form rectangle regions with an area of 44.8, 11.2, 35.2, and 8.8 km^2 respectively. This indicates that the agents covered these sub-regions and found the targets within them. This is a significant achievement as it demonstrates that the mission segregation strategy efficiently searches large areas for targets and reduces uncertainty.

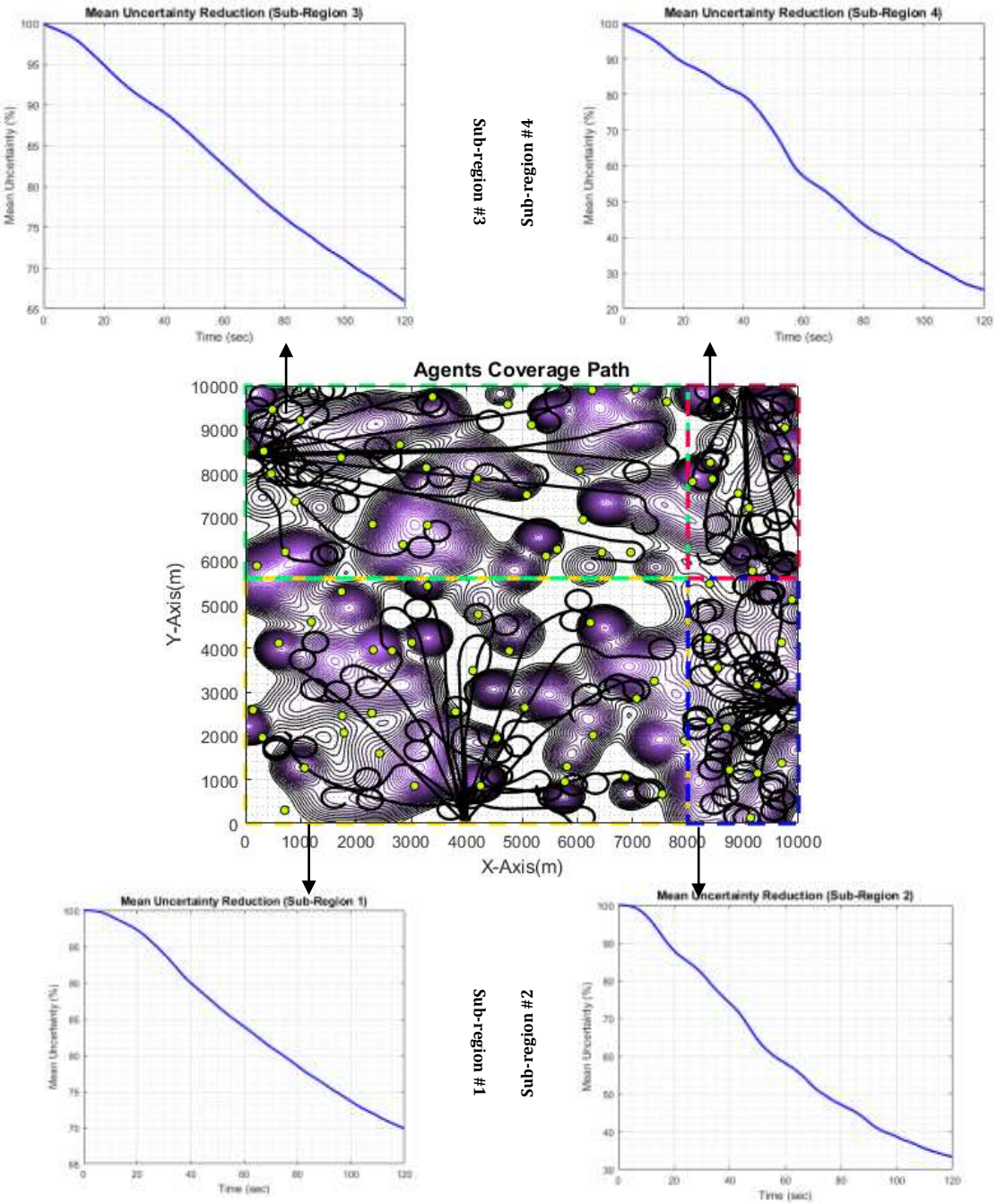

Figure 6. Proposed Strategy: Agent's path and Mean uncertainty reduction.

The simulation that covers the entire area without any mission segregation is an essential tool in assessing and verifying the performance of a strategy. The primary goal of this comparison is to ensure that the proposed strategy (implemented in the previous simulation) is effective in achieving its intended goals. This simulation provides a precise comparison with the previous simulation, as the number of agents used in both simulations is kept the same. Moreover, flight height and velocity are also kept constant to ensure that all parameters are considered similar to the previous simulation. By implementing this comparison, we can gain valuable insights into how well our proposed strategy works in practice.

The simulation results presented in Figure 7 demonstrate the superiority of the proposed approach over the existing approach in terms of coverage and target detection. While the existing approach was only able to reduce the uncertainty of the environment by 12.99 %, the proposed

approach achieved a remarkable 53.89% reduction in uncertainty. This significant difference in performance highlights the importance of adopting advanced techniques, such as the proposed approach, in multi-agent systems.

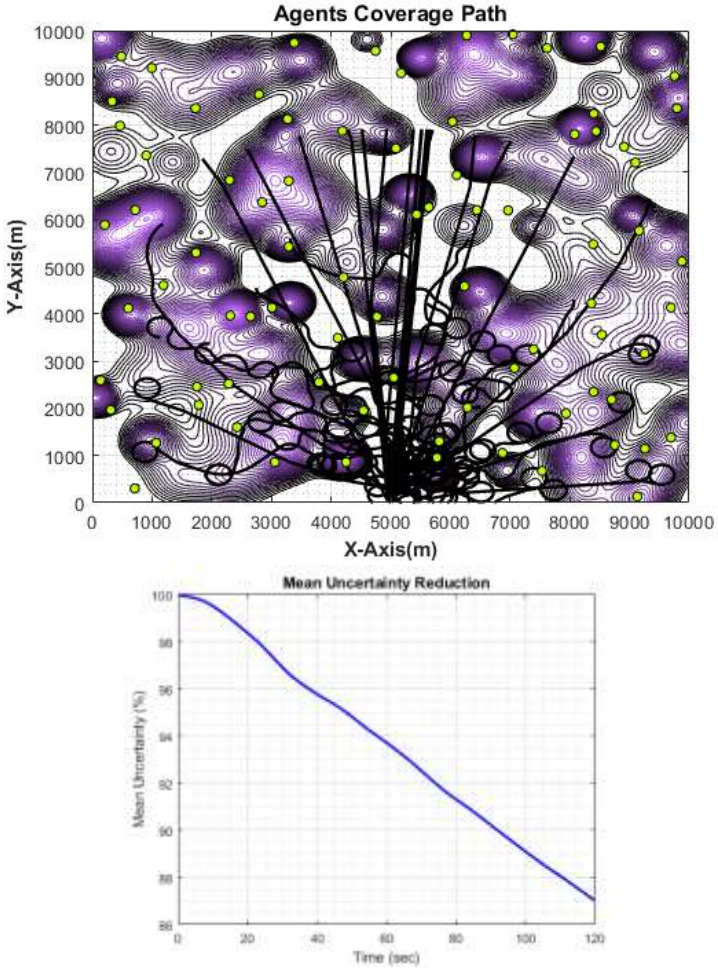

Figure 7. Agent's path and Mean uncertainty reduction.

Conclusion

This paper presents an optimal strategy for enhancing the performance of multi-agent systems by implementing cooperative search and coverage in uncertain environments. However, operational constraints such as time, number of agents, and dimensions of the surveillance region can significantly impact the efficiency of a multi-agent system. Therefore, it is crucial to optimize the performance of a multi-agent team within a given time frame while ensuring all constraints are satisfied. To address this issue, we propose an optimal strategy for mission segregation that can increase the performance of multi-agent systems while considering how operational parameters can affect system performance. The proposed strategy involves dividing a single mission into several simultaneous missions based on the optimal division of the environment. This creates a trade-off that ensures system performance optimality while achieving a common goal. The mission region is divided into sub-regions, and each sub-region is assigned to specific agents to improve overall system performance. The effectiveness of the proposed strategy is demonstrated through simulations and relevant comparisons. The results show that the proposed approach outperforms existing methods in terms of efficiency and effectiveness. Future work could involve applying this strategy to other multi-agent tasks/missions and exploring its potential in real-world scenarios. Overall, the proposed optimal strategy for mission segregation provides a practical solution for improving the performance of multi-agent systems in uncertain environments with operational limitations.

Conflicts of Interest

The authors of this paper declared no conflict of interest regarding the authorship or publication of this article.

References

[1]. Ru, C.J., Qi, X.M. and Guan, X.N., 2015. Distributed cooperative search control method of multiple UAVs for moving target. *International Journal of Aerospace Engineering*, *2015*. https://doi.org/10.1155/2015/317953

[2]. Mirzaei, M., Sharifi, F., Gordon, B.W., Rabbath, C.A. and Zhang, Y.M., 2011, December. Cooperative multi-vehicle search and coverage problem in uncertain environments. In *2011 50th IEEE Conference on Decision and Control and European Control Conference* (pp. 4140-4145). IEEE. https://doi.org/10.1109/CDC.2011.6161448

[3]. Sharifi, F., Mirzaei, M., Zhang, Y. and Gordon, B.W., 2015. Cooperative multi-vehicle search and coverage problem in an uncertain environment. *Unmanned systems*, *3*(01), pp.35-47. https://doi.org/10.1142/S230138501550003X

[4]. Durrant-Whyte, H. and Henderson, T.C., 2016. Multisensor data fusion. In *Springer handbook of robotics* (pp. 867-896). Springer, Cham. https://doi.org/10.1007/978-3-319-32552-1_35

[5]. Yang, Y., Polycarpou, M.M. and Minai, A.A., 2007. Multi-UAV cooperative search using an opportunistic learning method. *Journal of Dynamic Systems, Measurement, and Control*, *129*(5), pp.716-728. https://doi.org/10.1115/1.2764515

[6]. Murphy, R.R., 1998. Dempster-Shafer theory for sensor fusion in autonomous mobile robots. *IEEE Transactions on robotics and automation*, *14*(2), pp.197-206. https://doi.org/10.1109/70.681240

[7]. Yang, Y., Minai, A.A. and Polycarpou, M.M., 2005, June. Evidential map-building approaches for multi-UAV cooperative search. In *Proceedings of the 2005, American Control Conference, 2005.* (pp. 116-121). IEEE. https://doi.org/10.1109/ACC.2005.1469918

[8]. Hu, J., Xie, L., Lum, K.Y. and Xu, J., 2012. Multiagent information fusion and cooperative control in target search. IEEE Transactions on Control Systems Technology, 21(4), pp.1223-1235. https://doi.org/10.1109/TCST.2012.2198650

[9]. Aggarwal, S. and Kumar, N., 2020. Path planning techniques for unmanned aerial vehicles: A review, solutions, and challenges. Computer Communications, 149, pp.270-299. https://doi.org/10.1016/j.comcom.2019.10.014

[10]. Flint, M., Polycarpou, M. and Fernández-Gaucherand, E., 2002. Cooperative path-planning for autonomous vehicles using dynamic programming. IFAC Proceedings Volumes, 35(1), pp.481-486. https://doi.org/10.3182/20020721-6-ES-1901.01305

[11]. Sanna, G., Godio, S. and Guglieri, G., 2021, June. Neural network based algorithm for multi-UAV coverage path planning. In 2021 International Conference on Unmanned Aircraft Systems (ICUAS) (pp. 1210-1217). IEEE. https://doi.org/10.1109/ICUAS51884.2021.9476864

[12]. Yue, W., Guan, X. and Wang, L., 2019. A novel searching method using reinforcement learning scheme for multi-uavs in unknown environments. Applied Sciences, 9(22), p.4964. https://doi.org/10.3390/app9224964

[13]. Chang, H., Chen, Y., Zhang, B. and Doermann, D., 2021. Multi-uav mobile edge computing and path planning platform based on reinforcement learning. IEEE Transactions on Emerging Topics in Computational Intelligence. https://doi.org/10.48550/arXiv.2102.02078

[14]. Zhang, B., Mao, Z., Liu, W. and Liu, J., 2015. Geometric reinforcement learning for path planning of UAVs. Journal of Intelligent & Robotic Systems, 77(2), pp.391-409. https://doi.org/10.1007/s10846-013-9901-z

[15]. Lanillos, P., Gan, S.K., Besada-Portas, E., Pajares, G. and Sukkarieh, S., 2014. Multi-UAV target search using decentralized gradient-based negotiation with expected observation. Information Sciences, 282, pp.92-110. https://doi.org/10.1016/j.ins.2014.05.054

[16]. Gan, S.K. and Sukkarieh, S., 2011, May. Multi-UAV target search using explicit decentralized gradient-based negotiation. In 2011 IEEE International Conference on Robotics and Automation (pp. 751-756). IEEE. https://doi.org/10.1109/ICRA.2011.5979704

[17]. Chen, Y.B., Luo, G.C., Mei, Y.S., Yu, J.Q. and Su, X.L., 2016. UAV path planning using artificial potential

field method updated by optimal control theory. International Journal of Systems Science, 47(6), pp.1407-1420. https://doi.org/10.1080/00207721.2014.929191

[18]. Sun, J., Tang, J. and Lao, S., 2017. Collision avoidance for cooperative UAVs with optimized artificial potential field algorithm. IEEE Access, 5, pp.18382-18390. https://doi.org/10.1109/ACCESS.2017.2746752

[19]. Roberge, V., Tarbouchi, M. and Labonté, G., 2012. Comparison of parallel genetic algorithm and particle swarm optimization for real-time UAV path planning. IEEE Transactions on industrial informatics, 9(1), pp.132-141. https://doi.org/10.1109/TII.2012.2198665

[20]. Zhang, W., Zhang, S., Wu, F. and Wang, Y., 2021. Path planning of UAV based on improved adaptive grey wolf optimization algorithm. IEEE Access, 9, pp.89400-89411. https://doi.org/10.1109/ACCESS.2021.3090776

[21]. Zhou, X., Gao, F., Fang, X. and Lan, Z., 2021. Improved bat algorithm for UAV path planning in three-dimensional space. IEEE Access, 9, pp.20100-20116. https://doi.org/10.1109/ACCESS.2021.3054179

[22]. Hou, K., Yang, Y., Yang, X. and Lai, J., 2021. Distributed cooperative search algorithm with task assignment and receding horizon predictive control for multiple unmanned aerial vehicles. IEEE Access, 9, pp.6122-6136. https://doi.org/10.1109/ACCESS.2020.3048974

[23]. Liu, Z., Gao, X. and Fu, X., 2018. A cooperative search and coverage algorithm with controllable revisit and connectivity maintenance for multiple unmanned aerial vehicles. Sensors, 18(5), p.1472. https://doi.org/10.3390/s18051472

[24]. Zhang, M., Song, J., Huang, L. and Zhang, C., 2017. Distributed cooperative search with collision avoidance for a team of unmanned aerial vehicles using gradient optimization. Journal of Aerospace Engineering, 30(1), p.04016064.

[25]. Hu, J., 2013. Information fusion and cooperative control for target search and localization in multi-agent sensor networks (Doctoral dissertation, Nanyang Technological University). https://doi.org/10.32657%2F10356%2F51879

[26]. Teruel, E., Aragues, R. and López-Nicolás, G., 2019. A distributed robot swarm control for dynamic region coverage. Robotics and Autonomous Systems, 119, pp.51-63. https://doi.org/10.1016/j.robot.2019.06.002

[27]. Mathews, G.M., Durrant-Whyte, H. and Prokopenko, M., 2009. Decentralised decision making in heterogeneous teams using anonymous optimisation. Robotics and Autonomous Systems, 57(3), pp.310-320. https://doi.org/10.1016/j.robot.2008.10.020

[28]. Deb, K., Pratap, A., Agarwal, S. and Meyarivan, T.A.M.T., 2002. A fast and elitist multiobjective genetic algorithm: NSGA-II. IEEE transactions on evolutionary computation, 6(2), pp.182-197. https://doi.org/10.1109/4235.996017

HOW TO CITE THIS ARTICLE:
Benyamin Ebrahimi, Jafar Roshanian, Ali Asghar Bataleblu,"*Optimal Strategy for Multi-agent Mission Segregation: Search and Coverage Application*", Journal of Aerospace Science and Technology, Vol 17, No1,2024, pp, 34-46
DOI: https://doi.org/10.22034/jast.2023.403842.1156
URL: https://jast.ias.ir/article_178939.html